

Accurate fundamental parameters of *CoRoT* asteroseismic targets

The solar-like stars HD 49933, HD 175726, HD 181420 and HD 181906

H. Bruntt¹

¹ Observatoire de Paris, LESIA, 5 place Jules Janssen, 92195 Meudon Cedex, France e-mail: bruntt@phys.au.dk

² Sydney Institute for Astronomy, School of Physics, University of Sydney, NSW 2006, Australia

Received February XXXX, 2009; accepted July YYYY, 2009

ABSTRACT

Context. The *CoRoT* satellite has provided high-quality light curves of several solar-like stars. Analysis of the light curves provides oscillation frequencies that make it possible to probe the interior of the stars. However, additional constraints on the fundamental parameters of the stars are important for the theoretical modelling to be successful.

Aims. We will estimate the fundamental parameters (mass, radius and luminosity) of the first four solar-like targets to be observed in the asteroseismic field. In addition, we will determine their effective temperature, metallicity and detailed abundance pattern.

Methods. To constrain the stellar mass, radius and age we use the SHOTGUN software which compares the location of the stars in the Hertzsprung-Russell diagram with theoretical evolution models. This method takes into account the uncertainties of the observed parameters including the large separation determined from the solar-like oscillations. We determine the effective temperatures and abundance patterns in the stars from the analysis of high-resolution spectra.

Results. We have determined the mass, radius and luminosity of the four *CoRoT* targets to within 5–10%, 2–4% and 5–13%, respectively. The quality of the stellar spectra determines how well we can constrain the effective temperature. For the two best spectra we get 1- σ uncertainties below 60 K and for the other two 100–150 K. The uncertainty on the surface gravity is less than 0.08 dex for three stars while for HD 181906 it is 0.15 dex. The reason for the larger uncertainty is that the spectrum has two components with a luminosity ratio of $L_p/L_s = 0.50 \pm 0.15$. While *Hipparcos* astrometric data strongly suggest it is a binary star we find evidence that the fainter star may be a background star, since it is less luminous but hotter.

Key words. Stars: fundamental parameters – Stars: individual: HD 49933, HD 175726, HD 181420, HD 181906

1. Introduction

One of the ultimate science goals of the asteroseismic investigation of the *CoRoT* mission is to compare the observed oscillation frequencies with theoretical pulsation models. This will in principle allow us to probe the inside of stars and in particular determine how well we think we understand the physics of stars. We can examine how well the models describe the observations and hopefully be able to improve some of the approximations that are necessary when computing theoretical models.

To be able to confront the theoretical models with the observations we need accurate and reliable estimates of the fundamental parameters of the stars, i.e. mass, radius and luminosity. In this present work we will discuss how these parameters can be estimated by comparison with theoretical evolution models. In addition, we determine the atmospheric parameters from photometric indices and detailed spectroscopic analysis of absorption lines to get the chemical composition. In particular, we will give results for four solar-like stars observed in the asteroseismic field of *CoRoT*: HD 49933, HD 175726, HD 181420 and HD 181906.

2. Observations

For the target HD 49933 we used spectra from a 10-day spectroscopic campaign with the HARPS spectrograph (Mosser et al. 2005). From their bisector analysis it was found that stellar activity was affecting the cores of the spectral lines and this varied from night to night. We stacked 49 spectra from the quiet period

Table 1. Properties of the observed spectra. The first column gives the abbreviation used for each spectrum. Also listed is the resolution of the spectrograph, the wavelength range used in the abundance analysis, the S/N in the continuum for the original resolution (column 5) and S/N₄₂ for a resolution of 42 000. The last column contains the measured $v \sin i$.

HD/Sp.	Spectro-graph	<i>R</i>	Range [Å]	S/N	S/N ₄₂	$v \sin i$ [km s ⁻¹]
49933/H-A	HARPS	115 000	4050–6850	400	740	10
/H-C	HARPS	115 000	4050–6850	430	790	–
175726/N	NARVAL	65 000	4150–8500	900	1110	12
/E	ELODIE	42 000	4050–6800	130	130	–
181420/F	FEROS	48 000	3800–8850	120	120	18
/E	ELODIE	42 000	4300–6800	120	120	–
181906/E	ELODIE	42 000	4450–6750	110	110	10

(labeled “H-C” in the following) and collected 2001 January 19–20 from UT-22h to UT-06h. We stacked 35 from a more active period (labeled “H-A”) collected the following night from UT-20h to UT-05h. The H-A and H-C spectra have signal-to-noise ratios (S/N) in the continuum of just over 400.

Spectra of HD 175726, HD 181420 and HD 181906 were obtained from the GAUDI database (Solano et al. 2005). These spectra were collected as preparation for the *CoRoT* mission with the ELODIE spectrograph mounted on the 1.93-m telescope at the Haute-Provence observatory. The typical S/N in these spectra is 120. Additional spectra of HD 175726 were ob-

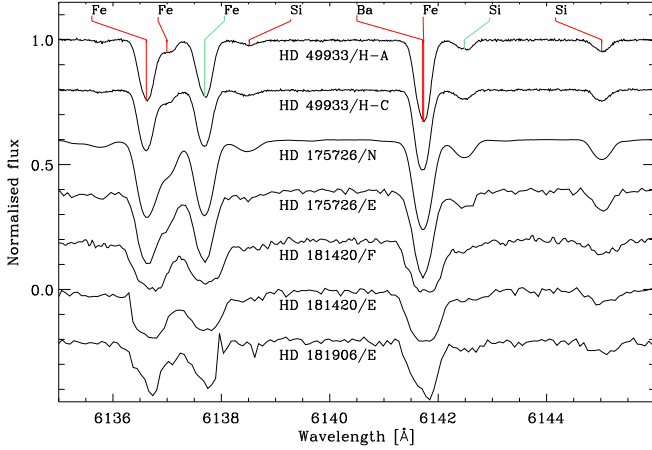


Fig. 1. A section of the observed spectra for the four stars (cf. Table 1). The absorption lines due to Fe, Si and Ba are marked.

tained with the NARVAL spectrograph on the 2m Bernard Lyot Telescope at the Pic du Midi observatory as part of the *CoRoT* follow-up program. We stacked 13 spectra to get a S/N of 900. A spectrum of HD 181420 was also obtained with the FEROS spectrograph at ESO.

A small section of the observed spectra is shown in Fig. 1 and the general properties of the spectra are listed in Table 1. The S/N was measured in the continuum as the average of several regions in the range 5 500–6 500 Å. We calculated S/N for the original resolution and when degraded to $R = 42\,000$ (S/N_{42} in Table 1) with two pixels per resolution element.

We determined the projected rotation velocity ($v \sin i$) by fitting synthetic spectra to several isolated lines while assuming a macroturbulence of 2 km s^{-1} for all stars. The uncertainty on $v \sin i$ is 5% except for HD 181906 which has two components in the spectrum, so the uncertainty is larger, $v \sin i = 10 \pm 1 \text{ km s}^{-1}$. Nordström et al. (2004) determined a much higher value of $v \sin i = 16 \text{ km s}^{-1}$, which we also get if we assume it is a single star. We shall discuss the possible binary nature of HD 181906 in Sect. 5. For the other three stars our $v \sin i$ values agree with Nordström et al. (2004) within the uncertainty, although we note that their values are all exactly 1 km s^{-1} higher.

3. Fundamental parameters of stars

The fundamental parameters of a star are its mass, M , radius, R , and luminosity, L . A direct measurement of mass can be done for the components in detached eclipsing binary systems with an accuracy of about 1–2 per cent (Andersen 1991) or for single stars in the rare case of a microlensing event (Alcock et al. 2001). The radius of single stars can be measured to about 1 per cent with interferometric methods or to about the same precision for eclipsing binary stars. The luminosity can be estimated from the V magnitude using the parallax and a bolometric correction, which is determined from model atmospheres.

For the relatively faint *CoRoT* asteroseismic targets we cannot apply these direct methods to get the mass and radius, so we must rely on indirect methods. An advantage for the solar-like *CoRoT* targets is that their density can be constrained from the large separation ($\Delta\nu$) which is measured to 2 per cent or better (Michel et al. 2008) from the oscillation frequencies.

More detailed investigations involve comparison of the individual observed frequencies with theoretical models. The aim of

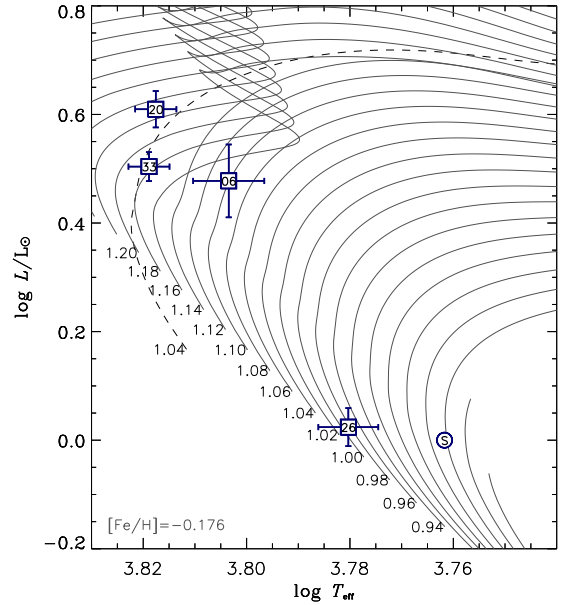


Fig. 2. Hertzsprung-Russell diagram showing the position of the four *CoRoT* stars. Full lines are evolution tracks from ASTEC for $[\text{Fe}/\text{H}] = -0.176$ and the dashed line is for $[\text{Fe}/\text{H}] = -0.480$. The uncertainties and location of each target is marked by a box and identified by the last two digits in the HD number. The mass is indicated for each track and the location of the Sun is marked with “S”.

this work is to estimate the parameters that are used by the theoreticians, namely L , effective temperature, T_{eff} , surface gravity, $\log g$, and the chemical composition. In this Section we shall discuss how the fundamental parameters of stars can be determined.

3.1. Surface gravity from M and R

The position of the four *CoRoT* targets are shown in the Hertzsprung-Russell (H-R) diagram in Fig. 2, where ASTEC evolution tracks from Christensen-Dalsgaard (2008) are overlaid. The position of the Sun is shown for reference. The mass and radius of a single field star can be estimated by comparing its properties to such theoretical evolution tracks.

We adopted the so-called SHOTGUN method which is described in detail in Stello et al. (2009). In brief, we construct 200 values for the four parameters (T_{eff} , L/L_{\odot} , $[\text{Fe}/\text{H}]$, $\Delta\nu$) with a mean value equal to our estimated values (see below) and a Gaussian random scatter equal to the uncertainty. For each of the 200 values we locate the closest matching grid point among the evolution tracks and the method saves the mass, radius and age. We finally calculate the mean value and the RMS value as our estimate of the 1σ uncertainty. The method uses the large separation to constrain the fundamental properties of the targets, and we assume that it scales with the Sun as $\Delta\nu/\Delta\nu_{\odot} = \sqrt{\rho/\rho_{\odot}}$, following the arguments by Kjeldsen & Bedding (1995). The inclusion of the large separation constrains the possible radii of the models as was discussed in detail by Stello et al. (2009).

Compared to the description of SHOTGUN in Stello et al. (2009) we have increased the number of random seed values from 100 to 200 and we have used both BASTI isochrones (Pietrinferni et al. 2004) and ASTEC evolution tracks Christensen-Dalsgaard (2008). We find that the results for the

Table 2. Fundamental parameters found from photometric indices.

HD	$V - K$ T_{eff}	Strömgren indices		
		T_{eff}	$\log g$	[Fe/H]
49933	6590 \pm 60	6630 \pm 90	4.30 \pm 0.15	-0.48 \pm 0.12
175726	6030 \pm 80	5980 \pm 90	4.68 \pm 0.15	-0.21 \pm 0.10
181420	6570 \pm 60	6660 \pm 90	4.16 \pm 0.15	-0.07 \pm 0.11
181906	6360 \pm 100	6430 \pm 90	4.31 \pm 0.15	-0.20 \pm 0.11

four targets agree within the 1- σ uncertainty for both sets of models. In the following we quote the results using the ASTEC evolution tracks, for which we have a denser model grid.

The four input parameters to SHOTGUN are estimated from:

- T_{eff} : The $V - K$ index (calibration from Masana et al. 2006).
- L/L_{\odot} : V from SIMBAD, *Hipparcos* parallax (van Leeuwen 2007), and bolometric correction (Bessell et al. 1998).
- [Fe/H]: Initial value from the Strömgren m_1 index and the final value from the abundance analysis.
- $\Delta\nu$: Results from *CoRoT* except for HD 175726.

For the $\Delta\nu$ values we used the most recent results from *CoRoT*. Appourchaux et al. (2008) analysed a 60-day light curve from *CoRoT* using different techniques and found $\Delta\nu = 85.9 \pm 0.15 \mu\text{Hz}$. Michel et al. (2008) presented preliminary results of the analysis of HD 181420 and HD 181906 and found $\Delta\nu = 77 \pm 2$ and $88 \pm 2 \mu\text{Hz}$, respectively. Finally, for HD 175726 we used $\Delta\nu = 97.2 \pm 0.5 \mu\text{Hz}$ from Mosser et al. (2009). This indicates a quite evolved star which is not in agreement with the location of the star in the H-R diagram. The detailed analysis of the oscillation frequencies show that the large separation is modulated with frequency (Mosser et al. 2009), so one should be cautious when using the scaling relation for $\Delta\nu$. We therefore decided not to use the $\Delta\nu$ value as input to SHOTGUN for HD 175726.

In Table 3 we list the fundamental parameters from SHOTGUN. The 1- σ uncertainty on the mass is 5–10%, radius 2–4% and luminosity to 5–13%. The surface gravity is computed as $\log g = \log(M/M_{\odot}) - 2 \log(R/R_{\odot}) + \log g_{\odot}$, and the results are listed in Table 5. The formal 1- σ uncertainty on $\log g$ is 0.06 dex or slightly less for the four targets. We note that our estimates of the uncertainties do not include the effects of changing the input physics of the models, e.g. mixing length, the equation of state or element diffusion. However, the more detailed investigation of Stello et al. (2009) shows that at least the radius is not significantly affected by changing these parameters.

3.2. The effective temperature

The effective temperature of a star, T_{eff} , is defined from the total flux per unit area from a black body: $\sigma T_{\text{eff}}^4 = F_{\text{tot}} = \int_0^{\infty} F_{\nu} d\nu = L/4\pi R^2$. To make a direct determination of T_{eff} one must measure F_{tot} from the angular diameter (from interferometry) and the flux integrated over all wavelengths (from spectrophotometry). This has been done recently for a few nearby solar-like asteroseismic targets (see North et al. 2007, 2009) and yield T_{eff} to about 50 K. Interferometric measurements of the relatively faint *CoRoT* targets ($V \simeq 5\text{--}8$) may be possible in the near future with the recently installed PAVO instrument at the CHARA array (Ireland et al. 2008) or AMBER at VLTI (Petrov et al. 2007).

When such measurements are not available, T_{eff} can be estimated by indirect methods, e.g. using the Balmer lines, calibration of line depth ratios, photometric colour indices and detailed abundance analyses (see Sect. 4). We did not use the

Table 3. Fundamental parameters of the *CoRoT* targets. The age, mass and radius was found using the SHOTGUN method. The luminosity is determined from V , the bolometric correction and the parallax.

HD	Age [Gyr]	M/M_{\odot}	R/R_{\odot}	L/L_{\odot}
49933	4.4 \pm 1.0	1.079 \pm 0.073	1.385 \pm 0.031	3.47 \pm 0.18
175726	4.8 \pm 3.5	0.993 \pm 0.060	1.014 \pm 0.035	1.210 \pm 0.064
181420	2.7 \pm 0.4	1.311 \pm 0.063	1.595 \pm 0.032	4.28 \pm 0.28
181906	4.2 \pm 1.6	1.144 \pm 0.119	1.392 \pm 0.054	3.29 \pm 0.43

Balmer lines due to the difficulty of normalising these lines that cover several spectral orders. The calibration of line-depth ratios of late F–K type stars was done by Kovtyukh et al. (2003), but the valid range is 4000–6150 K, and could thus only be used for the coolest star in our sample, HD 175726 (see Kovtyukh et al. 2004). Several calibrations of photometric indices exist in the literature, e.g. for F- and G-type main sequence stars the $V - K$ index (Masana et al. 2006) and Strömgren indices (Ramírez & Meléndez 2005) have recently been calibrated. The $V - K$ index has the advantage that it is less sensitive to interstellar reddening and in the following we have adopted the T_{eff} obtained from this index as our initial value for SHOTGUN and the abundance analyses.

We used the Strömgren indexes from Hauck & Mermilliod (1998) as input to the TEMPLOGG (Rogers 1995; Kupka & Bruntt 2001) software¹ to investigate if any of the stars have significant interstellar reddening. This requires the H_{β} index, which has not been measured for HD 175726. For HD 49933, HD 181420 and HD 181906 we find slightly negative values for $E(b - y)$, although they are consistent with zero within the uncertainties. The distance to the four *CoRoT* stars range from 26–68 parsec and in the following we assume that the targets have interstellar reddening close to zero, i.e. $E(b - y) = 0.000 \pm 0.005$. This corresponds to an uncertainty on T_{eff} of 50 K which we include in our estimates of T_{eff} from the photometric indices.

In Table 2 we give the results using the photometric indices. We used 2MASS $V - K$ from Cutri et al. (2003) to get T_{eff} using the calibration of Masana et al. (2006). We also list T_{eff} using the Strömgren calibration of Ramírez & Meléndez (2005). There is a very good agreement on the T_{eff} determined from the photometric indices. The T_{eff} determined from line depth ratios for HD 175726 is 6036 \pm 15 K (Kovtyukh et al. 2004; internal error is quoted) and this is fully consistent with the photometric calibrations. In Table 2 we also list $\log g$ from TEMPLOGG and [Fe/H] using the Strömgren calibration from Martell & Laughlin (2002) (see below).

3.3. Metallicity

The metallicity of F- and G-type stars has been calibrated through the Strömgren m_1 index, which measures the strength of metal lines in a narrow band around 400–420 nm. The calibration has recently been revised by Martell & Laughlin (2002) and the 1- σ scatter of their calibration is 0.09 dex. To this we add the internal scatter assuming that each photometric index ($b - y$, c_1 , m_1) has a 1- σ uncertainty of 0.005. The results are given in the last column in Table 2.

A more detailed view of the composition of stars is found from abundance analysis of individual spectral absorption lines

¹ On line version: <http://www.univie.ac.at/asap/templogg/main.php>

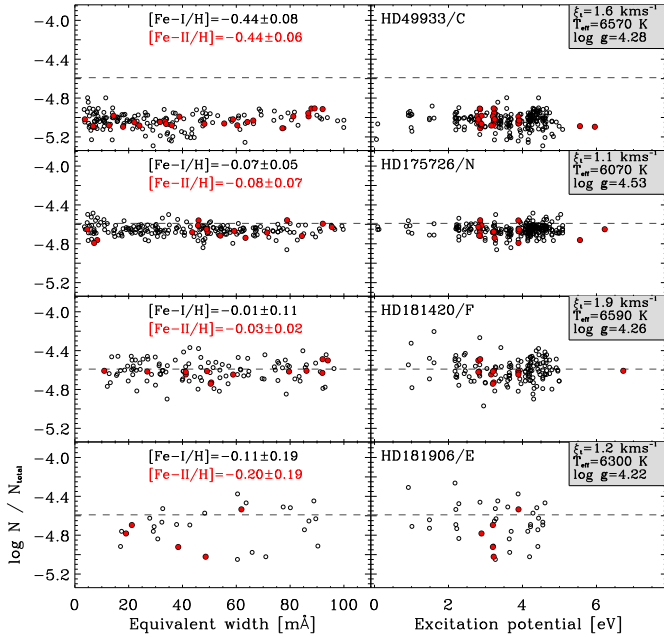


Fig. 3. Abundance determined for Fe lines versus equivalent width and excitation potential. Results are shown for the best spectrum available for the four targets. Open and solid circles are for neutral and ionised lines, respectively. The dashed lines mark the abundance in the Sun.

formed in the photosphere of the star. It is important to realise that we can only assume that this represents the global chemical composition of the star. Diffusion processes and element levitation are important in some stars and will change the radial distribution of elements. When modelling stars the chemical composition is often parametrised in terms of the mass fractions of hydrogen (X), helium (Y) and the rest is “heavy elements” (Z). From spectroscopy of solar-type stars we cannot constrain the helium content. Carbon, nitrogen and oxygen each give a significant contribution to Z . Therefore, it is important to obtain spectra that cover the near infrared where some carbon and oxygen lines are found (i.e. the spectra we have from FEROS and NARVAL).

The results of abundance analyses rely on the adopted model atmospheres that depend on T_{eff} , $\log g$, $[\text{Fe}/\text{H}]$, and microturbulence (ξ_t). A detailed analysis requires a good spectrum, say $S/N > 150$ and covering 1000 \AA or more in the optical range ($4000\text{--}7000 \text{ \AA}$). These data are easily obtained for the *CoRoT* targets – both in the asteroseismic field and the planet field – although for the faintest planet-hosting stars large telescopes are needed to get the required S/N . For slowly rotating stars ($v \sin i < 25 \text{ km s}^{-1}$) the metallicity can be determined to 0.05 dex, provided the atmospheric parameters are constrained to better than 100 K and 0.1 dex for T_{eff} and $\log g$, respectively. We will discuss the uncertainties in more detail and describe our method and results in the next Section.

4. Detailed spectral analysis with VWA

To analyse the spectra listed in Table 1 we used the software package VWA, which has been described in detail by Bruntt et al. (2004, 2008). The software uses atomic data from the VALD database (Kupka et al. 1999) and interpolation of atmospheric models either from a modified ATLAS9

grid (Heiter et al. 2002) or the MARCS grid (Gustafsson et al. 2008). In the current study we have used the MARCS grid which implements the recently updated abundances in the Sun (Grevesse et al. 2007).

We first analysed the solar spectrum from Hinkle et al. (2000), originally published by Kurucz et al. (1984). We used a model atmosphere with $T_{\text{eff}} = 5777 \text{ K}$, $\log g = 4.44$, $[\text{Fe}/\text{H}] = 0.0$ and $\xi_t = 1.0 \text{ km s}^{-1}$, interpolated in the same grid as used for the four *CoRoT* stars. We determined abundances for 1413 lines in the solar spectrum in the range 3777 to 9290 \AA using the VALD oscillator strengths ($\log gf$). We next adjusted the $\log gf$ values so each line gives the same abundance as in Grevesse et al. (2007). Only lines with adjusted $\log gf$ values were used in the analysis of the *CoRoT* targets. In Tables A.1–A.3 we list the line parameters (on-line material). This purely differential analysis was also used by Bruntt et al. (2008) who discussed the approach in more detail. As a test of the robustness of method we analysed three other solar spectra obtained with HARPS² (Mayor et al. 2003) which have a resolution, wavelength coverage and S/N comparable to the best *CoRoT* spectra. We find that the determined T_{eff} , $\log g$ and individual abundances are consistent with the Sun within the uncertainties (for more details on this analysis see Bruntt et al. 2009, in preparation).

In the first step of the analysis, VWA automatically identifies isolated lines in the spectrum and fits them iteratively using the initial values of T_{eff} , $\log g$, and metallicity from the photometric indices. By analysing the correlations of neutral Fe lines with equivalent width (EW) and excitation potential (EP) the T_{eff} and ξ_t are automatically adjusted. Similarly, VWA requires that abundances of neutral and ionised Fe lines give the same abundance³, which is adjusted by changing primarily $\log g$. Changes in T_{eff} also modify the ionisation balance, i.e. the resulting T_{eff} and $\log g$ are correlated. For the stars we have analysed an adjustment of T_{eff} of $+100 \text{ K}$ can be compensated by a change in $\log g$ of $+0.1$ dex. However, this degeneracy is partially lifted when the quality of the data is good.

To evaluate the uncertainties of the atmospheric parameters we repeat the analysis while perturbing T_{eff} , $\log g$ and ξ_t . From this we can determine when the correlations with EW and EP become significant or the ionisation balance begins to deviate (for details see Bruntt et al. 2008). We emphasise that this way of evaluating the uncertainties gives only an internal estimate since the absolute temperature scale of the model atmospheres may be systematically wrong. In other words, our results may indicate a good precision of T_{eff} and $\log g$, but the accuracy is most likely not as good. To evaluate the true accuracy we are currently undertaking the analysis of stars (Bruntt et al. 2009, in preparation) for which T_{eff} and $\log g$ are determined by methods that are only weakly model dependent (using interferometry and modelling of eclipsing binary stars). The preliminary results from this investigation indicate that the uncertainties given in current work are realistic.

Rentzsch-Holm (1996) have investigated the effects of non-LTE on Fe abundances which is important for stars earlier than F type, especially for stars more metal poor than the Sun. Her calculations show that Fe I is affected while Fe II is nearly unaffected. As a consequence, the ionisation balance is shifted relative to results from our applied LTE atmosphere models and it is therefore necessary to make adjustments in $\log g$ (Bruntt et al.

² <http://www.eso.org/sci/facilities/lasilla/instruments/harps/inst/monitoring/sun.html>

³ In the following we call this the “ionisation balance”, which is the difference in abundance: $A(\text{Fe II}) - A(\text{Fe I})$

Table 4. Atmospheric parameters determined with VWA. The first column lists the HD number and the spectrum used (cf. Table 1). In the analysis of HD 181906 $\log g$ could not be determined.

HD/Sp.	T_{eff} [K]	$\log g$	[Fe/H]	ξ_t [km/s]
49933/H-A	6560±110	4.28±0.05	-0.44±0.05	1.67±0.06
49933/H-C	6570±70	4.28±0.05	-0.44±0.04	1.60±0.10
175726/N	6070±45	4.53±0.04	-0.07±0.03	1.10±0.05
175726/E	6000±85	4.29±0.10	-0.09±0.05	1.07±0.11
181420/F	6590±130	4.26±0.07	-0.01±0.08	1.91±0.15
181420/E	6565±180	4.27±0.10	+0.02±0.11	1.69±0.10
181906/E	6300±150		-0.11±0.14	1.20±0.15

2008). We refer to Collet et al. (2005) (and references therein) for a recent discussion of the effects of UV line blocking on non-LTE calculations for Fe. Extrapolating from Figs. 4 and 5 in Rentzsch-Holm (1996) we find a correction of +0.05 dex for Fe I in HD 49933, which is the hottest and most metal poor star in our sample. HD 181420 has a T_{eff} similar to HD 49933 but it is more metal rich, so we estimate the correction to be +0.03 dex. The adjustment of $\log g$ needed to get ionisation balance is about twice these corrections ($\Delta \log g = +0.10$ and $+0.06$ dex, respectively). Since we have used extrapolations of the work by Rentzsch-Holm (1996) this leads to an additional uncertainty on $\log g$. We have therefore added 0.05 to the uncertainty on $\log g$ from VWA for HD 49933 and HD 181420.

In Fig. 3 we show the abundances of Fe in the best spectrum for each of the four stars. The abundances are shown versus equivalent width and excitation potential. Open circles are Fe I and solid circles are Fe II lines. The horizontal dashed lines mark the solar abundance. The mean abundance and RMS scatter of Fe I and Fe II lines are given in each panel. The results for the other spectra listed in Table 1 give similar results, but the overall scatter is larger.

We have checked whether the Fe abundances are correlated with other atomic line parameters. For HD 175726 and HD 181906 we find a significant correlation with wavelength. For HD 175726 this is especially true for the ELODIE spectrum, while it is less evident in the HARVAL spectrum. This could be an indication of problems with the subtraction of scattered light during the reduction of the ELODIE spectrum. For HD 181906 there is a strong correlation of Fe I and wavelength. From close inspection of the observed and synthetic spectra we see a clear asymmetry in the observed line profiles due to the contamination of light from another star. We shall discuss the detailed analysis of this star in Sect. 5.

The atmospheric parameters we determine for each spectrum are given in Table 4. For our final result we have computed the weighted mean values and they are listed in Table 5. For the reason stated above the result for the HD 175726/E spectrum was rejected. The $\log g$ determined from spectroscopy is systematically 0.1 dex higher than determined from the SHOTGUN method, and we will investigate this in future work. In Table 5 we also compare our results with values found in the literature. There is quite good agreement except for a few cases. For HD 49933 Kallinger et al. (2008) found $\log g = 3.9 \pm 0.1$, which is significantly lower than the other determinations. For HD 175726 Gillon & Magain (2006) found a significantly higher T_{eff} and $\log g$. They used the same ELODIE spectrum that we rejected. Also, as we have discussed, T_{eff} and $\log g$ are correlated and this could be an example of this problem (see also Sect. 6.2 in Bruntt et al. 2008).

Table 5. Fundamental parameters from this study and the literature.

HD	T_{eff}	$\log g$	[Fe/H]	Source
49933	6570±60	4.28 ±0.06	-0.44±0.03	VWA
	6630±90	4.30 ±0.15	-0.48±0.12	Strömgren
		4.189±0.035		SHOTGUN
	6450±75	3.9 ±0.1		Kallinger (2009)
	6780±130	4.24 ±0.13	-0.46±0.08	Bruntt (2008)
	6598±60	4.08 ±0.2	-0.29±0.1	Cenarro et al. (2007)
	6735±53	4.26 ±0.08	-0.37±0.03	Gillon (2006)
175726	6780±70	4.3 ±0.2	-0.30±0.11	Bruntt (2004)
	6070±45	4.53 ±0.04	-0.07±0.03	VWA
	5980±90	4.68 ±0.15	-0.21±0.10	Strömgren
		4.424±0.040		SHOTGUN
	5998±44	4.41 ±0.06	-0.10±0.03	Valenti (2005)
	6036±15	4.40	-0.12	Kovtyukh (2004)
	6217±32	4.61 ±0.04	+0.03±0.03	Gillon (2006)
181420	6580±105	4.26 ±0.08	+0.00±0.06	VWA
	6660±90	4.16 ±0.15	-0.07±0.11	Strömgren
		4.151±0.027		SHOTGUN
181906	6300±150		-0.11±0.14	VWA
	6430±90	4.31 ±0.15	-0.20±0.11	Strömgren
		4.220±0.056		SHOTGUN

The abundances in the four *CoRoT* targets are given in Table 6 and the abundance pattern is shown in Fig. 4. For each of the 17 elements the result is given from left to right for HD 49933, HD 175726, HD 181420 and HD 181906. The open and solid circles are the mean abundances determined from neutral and ionised lines, respectively. To be able to show the results on the same scale we plot all abundances relative to the Fe I abundance in each star. The uncertainty on the abundances includes contributions from the error on the mean value and the contribution from the uncertainty on the atmospheric parameters. When only one or two lines are available we assume an uncertainty of 0.1 dex. We have not included hyperfine structure levels for Mn and this probably explains the apparent underabundance of this element.

Abundance analyses of two of the stars are found in the literature. Valenti & Fischer (2005) published a homogeneous set of fundamental parameters for 1,040 FGK-type stars with spectra from radial velocity surveys to find exoplanets. They used synthetic spectra to determine T_{eff} , $\log g$, and abundances of Na, Si, Ti, Fe and Ni. Only HD 175726 is included in their study and they find the star to have an overall metallicity of $[M/H] = -0.10$. Our results agree remarkably well for the individual six elements with the largest difference being 0.03 dex. Gillon & Magain (2006) analysed HD 49933 and HD 175726. Our results are in acceptable agreement for HD 49933 while for HD 175726 the results disagree. The differences can be explained by the higher T_{eff} and $\log g$ determined by Gillon & Magain (2006). Finally, Kallinger et al. (2008) also analysed HARPS spectra of HD 49933 but they found evidence that only Fe is underabundant while carbon and oxygen are close to the solar value. Our abundance for carbon is based only two lines, but does not confirm this result.

5. The binary nature of HD 181906

Examples of lines fitted by VWA for HD 181906 are shown in Fig. 5. The observed profiles show an asymmetry due to the contamination of a fainter star in the blue wing of the absorption lines. We have recently expanded VWA to be able to analyse

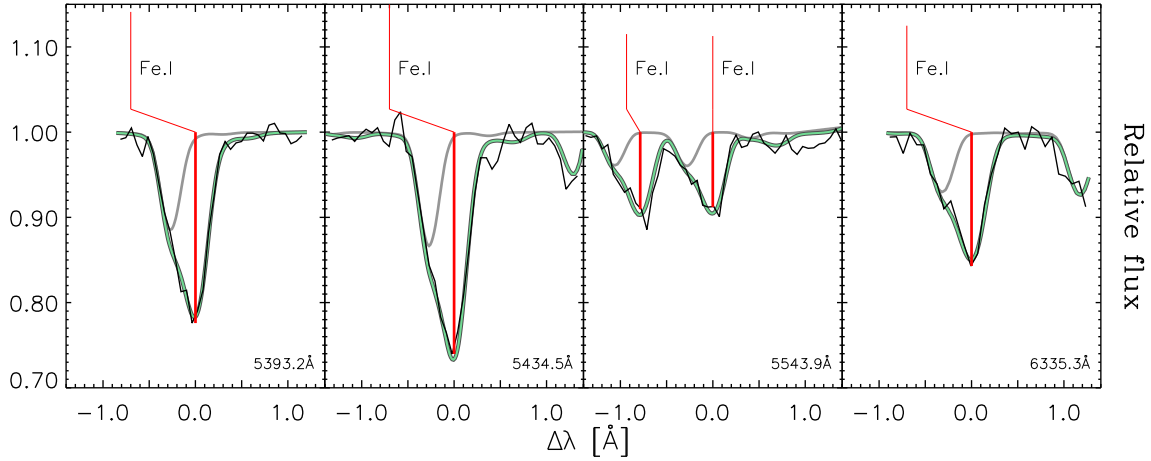


Fig. 5. Examples of four Fe I lines fitted by VWA for HD 181906. The observed lines (black) are asymmetric due to the contribution from a fainter star in the blue wing of the lines. The contribution to the spectrum from the contaminating star is taken into account in the analysis. The synthetic spectrum for the faint star is shown in grey and the combined spectrum is shown in green.

Table 6. Abundances relative to the Sun for the four *CoRoT* targets.

	HD 49933/H-C	HD 175726/N	HD 181420/F	HD 181906
C I	-0.58	2 -0.26±0.14	3 -0.13±0.25	4
O I		-0.09±0.03	3 +0.15	2
Na I	-0.40±0.06	3 -0.19±0.03	3 +0.17	2
Mg I	-0.47	1 -0.06	1 -0.16	2
Al I		-0.13	1 +0.09	2
Si I	-0.43±0.06	10 -0.13±0.03	16 -0.04±0.08	7
Si II	-0.35±0.05	2	+0.10	1
S I	-0.40	1 -0.14	1 +0.00	2
Ca I	-0.39±0.06	11 -0.01±0.03	3 +0.02±0.08	12 +0.14±0.10 4
Sc II	-0.46±0.06	5 -0.12±0.04	5 +0.01±0.09	4
Ti I	-0.37±0.06	13 -0.04±0.04	13 +0.08	2
Ti II	-0.40±0.06	11 -0.09±0.03	12 -0.15±0.10	3 -0.21 1
V I	-0.53	1 -0.07±0.04	8	
Cr I	-0.49±0.06	12 -0.09±0.03	18 -0.04±0.08	5 -0.19 2
Cr II	-0.44±0.09	3 -0.08±0.06	4 -0.19	1 -0.18±0.12 4
Mn I	-0.88±0.07	9 -0.26±0.03	4 -0.35±0.11	3 -0.28±0.24 3
Fe I	-0.49±0.05	193 -0.08±0.03	232 -0.05±0.07	141 -0.10±0.10 37
Fe II	-0.43±0.06	23 -0.05±0.03	15 +0.00±0.07	18 -0.18±0.12 6
Co I	-0.50	1 -0.20	1	
Ni I	-0.52±0.06	29 -0.19±0.03	46 -0.10±0.08	28 -0.43±0.12 8
Y II	-0.47±0.07	2 +0.03	1 +0.01±0.28	2

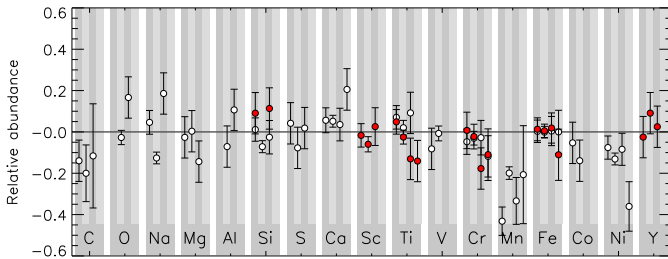


Fig. 4. Abundance pattern in the four target stars for 17 elements. For each element the result is given from left to right for HD 49933, 175726, 181420 and 181906. Open circles are the mean abundances determined from neutral lines and solid circles are for singly ionised lines. To show the patterns on the same scale all elements are offset relative to the abundance of Fe I.

binary stars, where each component has a different atmospheric model, line list and chemical composition (Clausen et al. 2008). We initially assumed the composite spectrum was a binary since Makarov & Kaplan (2005) and Frankowski et al. (2007) have found strong evidence for this based on *Hipparcos* astrometric data.

Due to the relatively weak lines in the fainter star, we assumed a low luminosity ratio ($R_L = L_p/L_s = 0.3$ at 6000 Å). For the secondary we initially assumed $T_{\text{eff}} = 5500$ K and $\log g = 4.4$ and for the primary we used T_{eff} from the $V - K$ index and $\log g$ from SHOTGUN. The values of $\log g$ were fixed throughout the analysis since not enough usable Fe II lines were available. VWA takes into account the change in R_L with wavelength while assuming Planck curves are valid representations of the variation of the flux with wavelength. We computed abundances for a grid for different assumptions of R_L and T_{eff} of the two components. Unfortunately, the S/N of the spectrum is quite poor and few lines are available. Therefore, the parameters of the secondary star cannot be determined very accurately. The best solution was found by minimising the correlations of Fe I with EW and EP (as for single stars) and the ionisation balance (only for the primary), and with the additional requirement that both stars have the same Fe abundance. We found $R_L = 0.50 \pm 0.15$ and for the secondary $T_{\text{eff}} = 6500 \pm 250$ K. Since the secondary is fainter but apparently a hotter star, we speculate that it is likely a background star rather than a part of a binary system. If this is true our assumption that the two stars have the same metallicity breaks down.

HD 181906 has the lowest power per oscillation mode of the four *CoRoT* stars analysed here (Michel et al. 2008). Our discovery that another relatively bright star is within the photometric aperture may partially explain this low amplitude. To investigate this possibility it is important to further constrain the parameters of the two stars, so we will acquire new spectra with high S/N.

6. Conclusion

We have determined the fundamental parameters of four solar-like stars observed with *CoRoT*. This work provides important input for the detailed theoretical modelling of the stars based on comparison with individual observed oscillation frequencies.

We described the SHOTGUN software from which the mass, radius and age are estimated by comparison with theoretical evolution tracks. The uncertainty on the mass is 5–10% and for the radius 2–4%. We can thus constrain $\log g$ better than 0.06 dex.

The luminosity was estimated using the updated parallaxes from van Leeuwen (2007) and the uncertainty lies in the range 5–13%. We determined T_{eff} from photometric indices and find excellent agreement with results from our detailed abundance analysis using high-S/N spectra. For the two stars with the highest S/N spectra (HD 49933 and HD 175726) we can constrain T_{eff} to within 60 K, which is better than through photometric indices. This is not the case for the two stars with relatively poor spectra (HD 181420 and HD 181906). We have determined the metallicity of the stars and the abundance pattern for up to 17 elements. Within the uncertainties the abundance pattern can be scaled from the Sun through the metallicity.

We found that the spectrum of HD 181906 consists of two components. From our analysis of the composite spectrum we obtain a luminosity ratio of $R_L = 0.50 \pm 0.15$. However, the fainter star appears to be hotter than the bright component. We therefore think the faint star may be a background star rather than being physically bound in a binary system. Further observations are needed to confirm this result.

Acknowledgements. This project was supported by the Australian and Danish Research Councils. We made use of the SIMBAD database, operated at CDS, Strasbourg, France. We used data from GAUDI, the data archive and access system of the ground-based asteroseismology programme of the *CoRoT* mission. The GAUDI system is maintained at LAEFF. LAEFF is part of the Space Science Division of INTA. We used atomic data extracted from the VALD data base made available through the Institute of Astronomy in Vienna, Austria. We thank C. Catala for providing the NARVAL spectrum of HD 175726.

References

- Alcock, C., Allsman, R. A., Alves, D. R., et al. 2001, *Nature*, 414, 617
- Andersen, J. 1991, *A&A Rev.*, 3, 91
- Appourchaux, T., Michel, E., Auvergne, M., et al. 2008, *A&A*, 488, 705
- Bessell, M. S., Castelli, F., & Plez, B. 1998, *A&A*, 333, 231
- Bruntt, H., Bikmaev, I. F., Catala, C., et al. 2004, *A&A*, 425, 683
- Bruntt, H., De Cat, P., & Aerts, C. 2008, *A&A*, 478, 487
- Cenarro, A. J., Peletier, R. F., Sánchez-Blázquez, P., et al. 2007, *MNRAS*, 374, 664
- Christensen-Dalsgaard, J. 2008, *Ap&SS*, 316, 13
- Clausen, J. V., Torres, G., Bruntt, H., et al. 2008, *A&A*, 487, 1095
- Collet, R., Asplund, M., & Thévenin, F. 2005, *A&A*, 442, 643
- Cutri, R. M., Skrutskie, M. F., van Dyk, S., et al. 2003, 2MASS All Sky Catalog of point sources. (NASA/IPAC Infrared Science Archive. <http://irsa.ipac.caltech.edu/applications/Gator/>)
- Frankowski, A., Jancart, S., & Jorissen, A. 2007, *A&A*, 464, 377
- Gillon, M. & Magain, P. 2006, *A&A*, 448, 341
- Grevesse, N., Asplund, M., & Sauval, A. J. 2007, *Space Sci. Reviews*, 130, 105
- Gustafsson, B., Edvardsson, B., Eriksson, K., et al. 2008, *A&A*, 486, 951
- Hauck, B. & Mermilliod, M. 1998, *A&AS*, 129, 431
- Heiter, U., Kupka, F., van't Veer-Menneret, C., et al. 2002, *A&A*, 392, 619
- Hinkle, K., Wallace, L., Valenti, J., & Harmer, D. 2000, *Visible and Near Infrared Atlas of the Arcturus Spectrum 3727-9300 Å* (San Francisco: ASP, USA)
- Ireland, M. J., Mérand, A., ten Brummelaar, T. A., et al. 2008, in *SPIE Conference Series*, Vol. 7013
- Kallinger, T., Gruberbauer, M., Guenther, D. B., Fossati, L., & Weiss, W. W. 2008, *ArXiv e-prints*
- Kjeldsen, H. & Bedding, T. R. 1995, *A&A*, 293, 87
- Kovtyukh, V. V., Soubiran, C., & Belik, S. I. 2004, *A&A*, 427, 933
- Kovtyukh, V. V., Soubiran, C., Belik, S. I., & Gorlova, N. I. 2003, *A&A*, 411, 559
- Kupka, F. & Bruntt, H. 2001, *First COROT/MONS/MOST Ground Support Workshop*, ed. C. Sterken (Vrije Universiteit Brussel, Belgium), 39
- Kupka, F., Piskunov, N., Ryabchikova, T. A., Stempels, H. C., & Weiss, W. W. 1999, *A&AS*, 138, 119
- Kurucz, R. L., Furenlid, I., Brault, J., & Testerman, L. 1984, *Solar flux atlas from 296 to 1300 nm* (National Solar Observatory Atlas, Sunspot, New Mexico, USA)
- Makarov, V. V. & Kaplan, G. H. 2005, *AJ*, 129, 2420
- Martell, S. & Laughlin, G. 2002, *ApJ*, 577, L45
- Masana, E., Jordi, C., & Ribas, I. 2006, *A&A*, 450, 735
- Mayor, M., Pepe, F., Queloz, D., et al. 2003, *The Messenger*, 114, 20
- Michel, E., Baglin, A., Auvergne, M., et al. 2008, *Science*, 322, 558
- Mosser, B., Bouchy, F., Catala, C., et al. 2005, *A&A*, 431, L13
- Mosser, B., Roxburgh, I., Michel, E., et al. 2009, *A&A*, submitted
- Nordström, B., Mayor, M., Andersen, J., et al. 2004, *A&A*, 418, 989
- North, J. R., Davis, J., Bedding, T. R., et al. 2007, *MNRAS*, 380, L80
- North, J. R., Davis, J., Robertson, J. G., et al. 2009, *MNRAS*, 393, 245
- Petrov, R. G., Malbet, F., Weigelt, G., et al. 2007, *A&A*, 464, 1
- Pietrinferni, A., Cassisi, S., Salaris, M., & Castelli, F. 2004, *ApJ*, 612, 168
- Ramírez, I. & Meléndez, J. 2005, *ApJ*, 626, 465
- Rentzsch-Holm, I. 1996, *A&A*, 312, 966
- Rogers, N. Y. 1995, *Communications in Asteroseismology*, 78, 1
- Solano, E., Catala, C., Garrido, R., et al. 2005, *AJ*, 129, 547
- Stello, D., Chaplin, W. J., Bruntt, H., et al. 2009, *ArXiv e-prints*
- Valenti, J. A. & Fischer, D. A. 2005, *ApJS*, 159, 141
- van Leeuwen, F. 2007, *A&A*, 474, 653

Appendix A: Lists of lines used in the abundance analysis

Table A.1. The atomic number, element name, wavelength, and $\log gf$ from the VALD database and the adjusted $\log gf$ value. The letters a–d indicate in which spectra the line was used in the analysis: a = HD 49933/H-C, b = HD 175726/N, c = 181420/F and d = HD181906/E.

El.	λ [Å]	VALD $\log gf$	Adjusted $\log gf$	Spectra	El.	λ [Å]	VALD $\log gf$	Adjusted $\log gf$	Spectra	El.	λ [Å]	VALD $\log gf$	Adjusted $\log gf$	Spectra
⁶ Ca I	4932.049	-1.884	-1.038	abc	Sc II	6245.637	-1.030	-1.053	ab	Cr II	5305.853	-2.357	-1.902	bd
Ca I	5380.337	-1.842	-1.452	a	Sc II	6604.601	-1.309	-1.258	abc	Cr II	5308.408	-1.846	-1.704	d
Ca I	5800.602	-2.338	-2.165	c	²² Ti I	4465.805	-0.163	-0.250	a	Cr II	5313.563	-1.650	-1.465	bd
Ca I	7113.179	-0.774	-0.658	bc	Ti I	4512.734	-0.480	-0.475	ab	²⁵ Mn I	4709.712	-0.340	-0.252	a
Ca I	7116.988	-0.907	-0.658	bc	Ti I	4534.776	+0.280	+0.225	b	Mn I	4754.042	-0.086	+0.358	abcd
⁸ O I	7771.941	+0.369	+0.784	b	Ti I	4548.763	-0.354	-0.401	a	Mn I	4761.512	-0.138	-0.079	a
O I	7774.161	+0.223	+0.627	bc	Ti I	4617.269	+0.389	+0.312	b	Mn I	4762.367	+0.425	+0.571	b
O I	7775.390	+0.001	+0.355	bc	Ti I	4623.097	+0.110	+0.079	b	Mn I	4766.418	+0.100	+0.306	ab
¹¹ Na I	5682.633	-0.700	-0.578	a	Ti I	4758.118	+0.425	+0.358	ab	Mn I	4783.427	+0.042	+0.434	abcd
Na I	5688.205	-0.450	-0.366	abc	Ti I	4759.270	+0.514	+0.445	c	Mn I	5377.637	-0.109	+0.179	a
Na I	6154.226	-1.560	-1.448	bc	Ti I	4820.411	-0.441	-0.498	ab	Mn I	5420.355	-1.462	-0.934	ab
Na I	6160.747	-1.260	-1.105	ab	Ti I	4928.336	+0.050	-0.160	a	Mn I	5537.760	-2.017	-1.904	a
¹² Mg I	4571.096	-5.691	-5.885	b	Ti I	4981.731	+0.504	+0.429	a	Mn I	6013.513	-0.251	+0.057	b
Mg I	5711.088	-1.833	-1.647	ac	Ti I	5016.161	-0.574	-0.530	b	Mn I	6021.819	+0.034	+0.213	acd
Mg I	8717.825	-0.930	-0.886	c	Ti I	5192.969	-1.006	-1.038	a	²⁶ Fe I	4080.209	-1.220	-1.285	a
¹³ Al I	6696.023	-1.347	-1.549	c	Ti I	5210.385	-0.884	-0.900	ab	Fe I	4080.877	-1.800	-1.827	a
Al I	6698.673	-1.647	-1.097	b	Ti I	5426.250	-3.006	-3.024	b	Fe I	4120.207	-1.267	-1.222	a
Al I	8772.865	-0.316	-0.233	c	Ti I	5866.451	-0.840	-0.929	a	Fe I	4136.521	-1.516	-1.456	a
¹⁴ Si I	5517.533	-2.384	-2.429	ab	Ti I	6258.102	-0.355	-0.411	ab	Fe I	4136.998	-0.453	-0.608	a
Si I	5645.613	-2.140	-2.005	a	Ti I	6258.706	-0.240	-0.329	ac	Fe I	4139.927	-3.629	-3.506	a
Si I	5666.677	-1.050	-1.598	a	Ti I	6261.098	-0.479	-0.512	ab	Fe I	4168.942	-1.650	-1.695	b
Si I	5675.417	-1.030	-1.039	c	Ti I	8434.957	-0.886	-0.802	b	Fe I	4184.892	-0.869	-0.851	ab
Si I	5684.484	-1.650	-1.551	b	Ti I	8435.652	-1.023	-1.031	b	Fe I	4199.095	+0.155	+0.029	a
Si I	5690.425	-1.870	-1.827	b	Ti II	4316.799	-1.580	-1.437	b	Fe I	4365.897	-2.250	-2.267	ab
Si I	5708.400	-1.470	-1.348	a	Ti II	4411.925	-2.550	-2.305	ab	Fe I	4389.245	-4.583	-4.522	a
Si I	5747.667	-0.780	-1.404	b	Ti II	4417.719	-1.230	-0.900	abc	Fe I	4432.568	-1.600	-1.736	b
Si I	5753.623	-0.830	-1.265	a	Ti II	4470.857	-2.060	-1.895	b	Fe I	4433.782	-1.267	-1.249	c
Si I	5793.073	-2.060	-1.936	b	Ti II	4493.513	-2.830	-2.775	a	Fe I	4438.343	-1.630	-1.679	b
Si I	5948.541	-1.230	-1.083	b	Ti II	4544.028	-2.530	-2.518	ab	Fe I	4439.881	-3.002	-3.007	ab
Si I	6091.919	-1.400	-1.251	c	Ti II	4589.958	-1.620	-1.446	abc	Fe I	4445.471	-5.441	-5.455	ab
Si I	6138.515	-1.350	-1.283	a	Ti II	4779.985	-1.260	-1.147	ab	Fe I	4480.137	-1.933	-1.818	b
Si I	6142.483	-0.920	-1.423	ab	Ti II	5129.152	-1.300	-1.005	b	Fe I	4485.676	-1.020	-1.096	abc
Si I	6145.016	-0.820	-1.356	bc	Ti II	5211.536	-1.356	-1.369	ac	Fe I	4489.739	-3.966	-3.951	b
Si I	6155.134	-0.400	-0.684	a	Ti II	5336.771	-1.630	-1.476	b	Fe I	4492.678	-1.650	-1.627	b
Si I	6237.319	-0.530	-0.967	ac	Ti II	5381.015	-1.970	-1.897	a	Fe I	4542.412	-2.050	-1.753	c
Si I	6244.466	-0.690	-1.222	b	Ti II	5418.751	-2.110	-1.997	abd	Fe I	4547.847	-1.012	-0.927	abc
Si I	6414.980	-1.100	-0.992	bc	Ti II	5490.690	-2.650	-2.660	a	Fe I	4551.647	-2.060	-1.928	b
Si I	6527.202	-1.500	-1.110	b	Ti II	6491.561	-1.793	-2.032	ab	Fe I	4587.128	-1.737	-1.671	abc
Si I	6635.687	-1.630	-1.816	a	Ti II	7575.423	-1.397	-1.327	b	Fe I	4595.359	-1.758	-1.612	b
Si I	6800.596	-1.640	-1.650	b	²³ V I	5627.633	-0.363	-0.588	b	Fe I	4602.001	-3.154	-3.197	abc
Si I	7405.772	-0.820	-0.632	b	V I	5670.853	-0.420	-0.571	b	Fe I	4602.941	-2.209	-2.188	abcd
Si I	7423.496	-0.314	-0.520	bc	V I	5727.048	-0.012	-0.137	b	Fe I	4607.647	-1.545	-1.210	ac
Si I	7918.384	-0.610	-0.409	b	V I	6039.722	-0.650	-0.810	b	Fe I	4625.045	-1.340	-1.396	abc
Si I	7932.348	-0.470	-0.216	b	V I	6090.214	-0.062	-0.268	b	Fe I	4630.120	-2.587	-2.561	ab
Si I	7944.001	-0.310	-0.056	c	V I	6119.523	-0.320	-0.566	b	Fe I	4635.846	-2.358	-2.349	ab
Si I	8443.970	-1.400	-1.285	b	V I	6199.197	-1.300	-1.606	b	Fe I	4637.503	-1.390	-1.285	ab
Si II	6347.109	+0.297	+0.506	a	V I	6243.105	-0.980	-1.117	ab	Fe I	4638.010	-1.119	-1.057	ab
Si II	6371.371	-0.003	+0.152	ac	²⁴ Cr I	4319.636	-0.820	-1.094	b	Fe I	4661.534	-1.270	-1.119	ab
¹⁶ S I	6052.674	-0.740	-0.483	c	Cr I	4545.945	-1.370	-1.446	b	Fe I	4661.970	-2.502	-2.361	b
S I	6757.171	-0.310	-0.208	abc	Cr I	4616.120	-1.190	-1.334	ab	Fe I	4669.171	-1.211	-1.156	b
²⁰ Ca I	4425.437	-0.286	-0.491	ac	Cr I	4626.174	-1.320	-1.414	ab	Fe I	4690.138	-1.645	-1.500	b
Ca I	4578.551	-0.170	-0.562	abd	Cr I	4651.282	-1.460	-1.496	abc	Fe I	4728.546	-1.172	-0.927	acd
Ca I	5349.465	-1.178	-0.256	b	Cr I	4652.152	-1.030	-0.916	abd	Fe I	4733.592	-2.988	-2.998	abcd
Ca I	5581.965	-0.569	-0.607	abcd	Cr I	4801.047	-0.131	-0.179	b	Fe I	4736.773	-0.752	-0.701	a
Ca I	5588.749	+0.313	+0.296	c	Cr I	4936.335	-0.340	-0.245	ab	Fe I	4741.530	-1.765	-1.940	ab
Ca I	5867.562	-0.801	-1.634	a	Cr I	5247.566	-1.640	-1.623	ab	Fe I	4745.800	-1.270	-1.102	abc
Ca I	6122.217	-0.386	-0.347	ac	Cr I	5287.200	-0.907	-0.921	b	Fe I	4757.582	-2.321	-1.958	b
Ca I	6166.439	-1.156	-1.161	bcd	Cr I	5296.691	-1.400	-1.375	abd	Fe I	4779.439	-2.020	-2.198	ab
Ca I	6169.042	-0.804	-0.814	a	Cr I	5297.376	+0.167	-0.014	abc	Fe I	4785.957	-1.930	-1.748	b
Ca I	6169.563	-0.527	-0.522	ac	Cr I	5300.744	-2.120	-2.153	bc	Fe I	4787.827	-2.530	-2.578	abc
Ca I	6439.075	+0.394	+0.370	cd	Cr I	5329.142	-0.064	-0.063	b	Fe I	4788.757	-1.763	-1.770	ab
Ca I	6449.808	-1.015	-0.480	a	Cr I	5348.312	-1.290	-1.238	abc	Fe I	4798.265	-1.174	-1.378	b
Ca I	6455.598	-1.557	-1.348	a	Cr I	5783.093	-0.500	-0.455	ab	Fe I	4799.406	-2.230	-2.115	a
Ca I	6471.662	-0.653	-0.668	cd	Cr I	5783.886	-0.295	-0.271	ab	Fe I	4802.880	-1.514	-1.519	bcd
Ca I	6493.781	+0.019	-0.107	bc	Cr I	5787.965	-0.083	-0.258	a	Fe I	4807.709	-2.200	-2.016	b
Ca I	6499.650	-0.719	-0.787	ac	Cr I	6661.078	-0.190	-0.165	b	Fe I	4809.938	-2.720	-2.550	a
Ca I	6717.681	-0.596	-0.474	acd	Cr I	7400.226	-0.111	-0.161	c	Fe I	4839.544	-1.822	-1.713	bd
Ca I	7326.145	+0.073	-0.049	a	Cr II	4554.988	-1.282	-1.356	a	Fe I	4886.326	-0.556	-0.547	ab
²¹ Sc II	5239.813	-0.765	-0.672	abc	Cr II	4616.629	-1.361	-1.160	ab	Fe I	4892.859	-1.290	-1.182	acd
Sc II	5526.790	+0.024	+0.069	abc	Cr II	4824.127	-0.970	-0.759	b	Fe I	4917.230	-1.180	-0.945	ab
Sc II	5669.042	-1.200	-1.072	abc	Cr II	5237.329	-1.160	-1.103	acd	Fe I	4924.770	-2.241	-2.085	ac

Table A.2. The atomic number, element name, wavelength, and $\log gf$ from the VALD database and the adjusted $\log gf$ value. The letters a–d indicate in which spectra the line was used in the analysis: a = HD 49933/H-C, b = HD 175726/N, c = 181420/F and d = HD181906/E.

El.	λ [Å]	VALD $\log gf$	Adjusted $\log gf$	Spectra	El.	λ [Å]	VALD $\log gf$	Adjusted $\log gf$	Spectra	El.	λ [Å]	VALD $\log gf$	Adjusted $\log gf$	Spectra
²⁶ Fe I	4930.315	-1.201	-0.956	abc	Fe I	5400.502	-0.160	-0.212	ab	Fe I	5856.088	-1.328	-1.582	abc
Fe I	4946.388	-1.170	-1.140	abc	Fe I	5401.269	-1.920	-1.701	ab	Fe I	5858.778	-2.260	-2.294	b
Fe I	4950.106	-1.670	-1.490	a	Fe I	5405.775	-1.844	-1.961	a	Fe I	5859.578	-0.398	-0.482	ac
Fe I	4962.572	-1.182	-1.098	abc	Fe I	5406.775	-1.720	-1.410	b	Fe I	5861.110	-2.450	-2.402	b
Fe I	4966.089	-0.871	-0.890	abcd	Fe I	5409.134	-1.300	-1.037	ab	Fe I	5862.353	-0.058	-0.158	ab
Fe I	4967.890	-0.622	-0.471	abd	Fe I	5415.199	+0.642	+0.427	acd	Fe I	5905.672	-0.730	-0.736	c
Fe I	4969.918	-0.710	-0.745	ac	Fe I	5424.068	+0.520	+0.559	a	Fe I	5916.247	-2.994	-2.956	bc
Fe I	4970.496	-1.740	-1.655	b	Fe I	5434.524	-2.122	-2.243	ad	Fe I	5927.789	-1.090	-1.092	b
Fe I	4973.102	-0.950	-0.821	abc	Fe I	5445.042	-0.020	-0.034	acd	Fe I	5929.677	-1.410	-1.149	b
Fe I	4977.647	-2.153	-1.958	ab	Fe I	5464.280	-1.402	-1.564	acd	Fe I	5930.180	-0.230	-0.221	ac
Fe I	4986.223	-1.390	-1.269	ab	Fe I	5466.396	-0.630	-0.611	abc	Fe I	5933.800	-2.230	-2.132	b
Fe I	4988.950	-0.890	-0.644	ab	Fe I	5466.988	-2.233	-2.273	ab	Fe I	5934.655	-1.170	-1.132	abc
Fe I	4994.130	-3.080	-3.187	abcd	Fe I	5470.094	-1.810	-1.565	b	Fe I	5952.718	-1.440	-1.345	b
Fe I	5014.943	-0.303	-0.302	b	Fe I	5472.709	-1.495	-1.500	ac	Fe I	5956.694	-4.605	-4.652	b
Fe I	5029.618	-2.050	-1.953	c	Fe I	5473.900	-0.760	-0.728	abc	Fe I	5976.775	-1.310	-1.131	c
Fe I	5044.211	-2.038	-2.089	bd	Fe I	5480.861	-1.260	-1.145	b	Fe I	5983.673	-1.878	-0.493	abcd
Fe I	5049.820	-1.355	-1.390	cd	Fe I	5481.243	-1.243	-1.257	b	Fe I	5984.814	-0.343	-0.045	b
Fe I	5054.643	-1.921	-1.983	a	Fe I	5487.145	-1.530	-1.375	ab	Fe I	5987.066	-0.556	-0.283	bc
Fe I	5068.766	-1.042	-1.186	b	Fe I	5497.516	-2.849	-2.996	b	Fe I	6003.012	-1.120	-1.030	abcd
Fe I	5072.668	-1.224	-0.815	b	Fe I	5506.779	-2.797	-2.918	ab	Fe I	6005.543	-3.192	-3.496	b
Fe I	5076.262	-0.767	-0.872	a	Fe I	5522.447	-1.550	-1.412	bc	Fe I	6007.960	-0.966	-0.551	a
Fe I	5083.339	-2.958	-3.086	ab	Fe I	5525.544	-1.084	-1.192	ab	Fe I	6008.554	-1.078	-0.764	abc
Fe I	5090.774	-0.400	-0.440	a	Fe I	5531.984	-1.610	-1.321	ab	Fe I	6024.058	-0.120	+0.013	abc
Fe I	5109.652	-0.980	-0.680	ac	Fe I	5543.936	-1.140	-1.016	abd	Fe I	6027.051	-1.089	-1.045	c
Fe I	5121.639	-0.810	-0.772	b	Fe I	5546.506	-1.310	-1.050	abc	Fe I	6034.035	-2.420	-2.314	b
Fe I	5127.359	-3.307	-3.346	ab	Fe I	5553.578	-1.410	-1.301	abc	Fe I	6035.338	-2.590	-2.620	b
Fe I	5131.469	-2.515	-2.379	a	Fe I	5560.212	-1.190	-1.030	abd	Fe I	6056.005	-0.460	-0.411	bc
Fe I	5133.689	+0.140	+0.210	ad	Fe I	5562.706	-0.659	-0.744	a	Fe I	6065.482	-1.530	-1.576	ac
Fe I	5137.382	-0.400	-0.300	b	Fe I	5565.704	-0.285	-0.001	ad	Fe I	6078.491	-0.424	-0.108	a
Fe I	5141.739	-1.964	-2.156	abc	Fe I	5567.391	-2.564	-2.770	ab	Fe I	6079.009	-1.120	-0.974	ab
Fe I	5145.094	-2.876	-3.191	ab	Fe I	5569.618	-0.486	-0.654	a	Fe I	6082.711	-3.573	-3.615	b
Fe I	5150.840	-3.003	-3.463	c	Fe I	5572.842	-0.275	-0.346	ac	Fe I	6085.259	-3.095	-2.983	ab
Fe I	5151.911	-3.322	-3.226	abcd	Fe I	5576.089	-1.000	-0.936	abc	Fe I	6093.644	-1.500	-1.334	ab
Fe I	5159.058	-0.820	-0.790	bcd	Fe I	5586.756	-0.120	-0.183	ac	Fe I	6094.374	-1.940	-1.564	b
Fe I	5194.942	-2.090	-2.279	ab	Fe I	5608.972	-2.400	-2.255	b	Fe I	6096.665	-1.930	-1.804	ab
Fe I	5195.468	-0.002	-0.081	ab	Fe I	5618.633	-1.276	-1.271	a	Fe I	6098.245	-1.880	-1.760	ab
Fe I	5196.077	-0.451	-0.636	a	Fe I	5619.595	-1.700	-1.440	abc	Fe I	6102.173	-0.627	-0.070	ab
Fe I	5198.711	-2.135	-2.175	abc	Fe I	5624.022	-1.480	-1.073	b	Fe I	6105.131	-2.050	-1.930	b
Fe I	5215.181	-0.871	-1.036	a	Fe I	5624.542	-0.755	-0.827	ac	Fe I	6127.907	-1.399	-1.367	abc
Fe I	5217.389	-1.070	-1.150	abcd	Fe I	5633.947	-0.270	-0.146	abc	Fe I	6136.615	-1.400	-1.476	c
Fe I	5228.377	-1.290	-1.061	c	Fe I	5635.823	-1.890	-1.567	abc	Fe I	6137.692	-1.403	-1.437	a
Fe I	5235.387	-0.854	-0.959	b	Fe I	5638.262	-0.870	-0.756	ab	Fe I	6151.618	-3.299	-3.338	ac
Fe I	5236.204	-1.497	-1.563	abc	Fe I	5641.434	-1.180	-1.066	a	Fe I	6157.728	-1.260	-1.117	a
Fe I	5242.491	-0.967	-0.953	ac	Fe I	5650.706	-0.960	-0.674	ab	Fe I	6165.360	-1.474	-1.446	abc
Fe I	5243.777	-1.150	-1.012	b	Fe I	5661.346	-1.736	-1.864	a	Fe I	6170.507	-0.440	-0.329	ab
Fe I	5247.050	-4.946	-4.992	b	Fe I	5677.685	-2.700	-2.646	b	Fe I	6173.336	-2.880	-2.897	abc
Fe I	5250.646	-2.181	-2.105	ac	Fe I	5679.023	-0.920	-0.717	bc	Fe I	6180.204	-2.586	-2.710	bc
Fe I	5253.462	-1.573	-1.631	abc	Fe I	5691.497	-1.520	-1.414	ab	Fe I	6187.990	-1.720	-1.644	ab
Fe I	5281.790	-0.834	-0.995	ac	Fe I	5696.090	-1.720	-1.890	b	Fe I	6200.313	-2.437	-2.404	ab
Fe I	5283.621	-0.432	-0.551	a	Fe I	5701.545	-2.216	-2.202	ab	Fe I	6213.430	-2.482	-2.586	abcd
Fe I	5285.129	-1.640	-1.495	ab	Fe I	5705.465	-1.355	-1.463	b	Fe I	6216.352	-1.425	-1.380	a
Fe I	5288.525	-1.508	-1.619	abd	Fe I	5717.833	-1.130	-0.993	ab	Fe I	6219.281	-2.433	-2.484	acd
Fe I	5293.959	-1.870	-1.701	ab	Fe I	5724.455	-2.640	-2.556	b	Fe I	6226.736	-2.220	-2.088	b
Fe I	5295.312	-1.690	-1.524	ab	Fe I	5731.762	-1.300	-1.098	b	Fe I	6229.228	-2.805	-2.942	ac
Fe I	5302.302	-0.720	-0.816	d	Fe I	5738.228	-2.340	-2.531	b	Fe I	6230.723	-1.281	-1.352	ac
Fe I	5307.361	-2.987	-3.052	bc	Fe I	5741.848	-1.854	-1.638	bc	Fe I	6232.641	-1.223	-1.112	abc
Fe I	5315.070	-1.550	-1.436	b	Fe I	5752.023	-1.267	-0.801	abd	Fe I	6246.319	-0.733	-0.828	acd
Fe I	5321.108	-0.951	-1.235	b	Fe I	5760.345	-2.490	-2.395	b	Fe I	6252.555	-1.687	-1.742	ac
Fe I	5322.041	-2.803	-2.994	bcd	Fe I	5762.992	-0.450	-0.364	b	Fe I	6265.134	-2.550	-2.561	ac
Fe I	5329.989	-1.189	-1.066	b	Fe I	5775.081	-1.298	-1.045	ab	Fe I	6270.225	-2.464	-2.589	b
Fe I	5361.625	-1.430	-1.277	abcd	Fe I	5780.600	-2.640	-2.465	ab	Fe I	6271.279	-2.703	-2.743	a
Fe I	5364.871	+0.228	+0.113	abc	Fe I	5793.915	-1.700	-1.626	b	Fe I	6330.850	-1.740	-1.179	abc
Fe I	5365.399	-1.020	-1.147	a	Fe I	5798.171	-1.890	-1.766	ab	Fe I	6335.331	-2.177	-2.336	acd
Fe I	5367.467	+0.443	+0.232	ad	Fe I	5806.725	-1.050	-0.872	ac	Fe I	6336.824	-0.856	-0.903	ac
Fe I	5373.709	-0.860	-0.776	abc	Fe I	5809.218	-1.840	-1.867	ac	Fe I	6338.877	-1.060	-0.870	b
Fe I	5379.574	-1.514	-1.474	ab	Fe I	5811.914	-2.430	-2.430	b	Fe I	6355.029	-2.350	-2.125	ac
Fe I	5383.369	+0.645	+0.450	acd	Fe I	5814.807	-1.970	-1.858	ab	Fe I	6380.743	-1.376	-1.252	abc
Fe I	5386.334	-1.770	-1.706	ab	Fe I	5845.287	-1.820	-1.896	b	Fe I	6393.601	-1.432	-1.596	ac
Fe I	5389.479	-0.410	-0.466	abc	Fe I	5848.123	-0.903	-1.184	abc	Fe I	6400.001	-0.290	-0.386	a
Fe I	5393.168	-0.715	-0.821	acd	Fe I	5852.219	-1.330	-1.244	bc	Fe I	6408.018	-1.018	-0.866	a
Fe I	5398.279	-0.670	-0.619	bc	Fe I	5855.077	-1.478	-1.564	b	Fe I	6411.649	-0.595	-0.670	ac

Table A.3. The atomic number, element name, wavelength, and $\log gf$ from the VALD database and the adjusted $\log gf$ value. The letters a–d indicate in which spectra the line was used in the analysis: a = HD 49933/H-C, b = HD 175726/N, c = 181420/F and d = HD181906/E.

El.	λ [Å]	VALD $\log gf$	Adjusted $\log gf$	Spectra	El.	λ [Å]	VALD $\log gf$	Adjusted $\log gf$	Spectra	El.	λ [Å]	VALD $\log gf$	Adjusted $\log gf$	Spectra
²⁶ Fe I	6419.950	-0.240	-0.266	c	Fe I	7807.952	-0.697	-0.461	bc	Ni I	4829.016	-0.330	-0.330	b
Fe I	6421.351	-2.027	-2.173	ab	Fe I	7832.194	+0.018	+0.202	b	Ni I	4831.169	-0.320	-0.388	c
Fe I	6430.846	-2.006	-2.109	abcd	Fe I	7941.089	-2.286	-2.476	b	Ni I	4904.407	-0.170	-0.234	abcd
Fe I	6436.407	-2.460	-2.350	b	Fe I	8028.309	-0.794	-0.677	c	Ni I	4935.831	-0.350	-0.317	ab
Fe I	6481.870	-2.984	-2.958	bc	Fe I	8046.047	-0.082	+0.177	b	Ni I	4953.200	-0.580	-0.835	ab
Fe I	6498.939	-4.699	-4.685	ab	Fe I	8207.745	-0.987	-0.843	b	Ni I	4998.218	-0.690	-0.845	ab
Fe I	6518.367	-2.460	-2.560	c	Fe I	8339.398	-1.421	-0.366	b	Ni I	5010.934	-0.870	-0.866	bc
Fe I	6592.914	-1.473	-1.601	ac	Fe I	8365.634	-2.047	-1.990	bc	Ni I	5017.568	-0.020	-0.168	a
Fe I	6593.870	-2.422	-2.374	ac	Fe I	8401.404	-3.442	-3.553	b	Ni I	5035.357	+0.290	+0.060	a
Fe I	6597.561	-1.070	-0.906	ac	Fe I	8439.563	-0.698	-0.672	b	Ni I	5081.107	+0.300	+0.184	ab
Fe I	6608.026	-4.030	-4.005	b	Fe I	8471.739	-0.863	-0.941	b	Ni I	5082.339	-0.540	-0.535	abcd
Fe I	6609.110	-2.692	-2.648	bc	Fe I	8514.072	-2.229	-2.239	b	Ni I	5084.089	+0.030	-0.090	b
Fe I	6627.545	-1.680	-1.485	b	Fe I	8582.257	-2.134	-2.086	c	Ni I	5094.406	-1.080	-1.108	a
Fe I	6633.750	-0.799	-0.721	ac	Fe I	8611.804	-1.926	-1.895	c	Ni I	5099.927	-0.100	-0.173	b
Fe I	6646.932	-3.990	-3.988	b	Fe I	8616.276	-0.405	-0.846	c	Ni I	5115.389	-0.110	-0.148	acd
Fe I	6677.987	-1.418	-1.455	ac	Fe I	8621.601	-2.321	-2.267	c	Ni I	5146.480	-0.060	-0.131	b
Fe I	6703.567	-3.160	-3.055	a	Fe I	8688.626	-1.212	-1.210	c	Ni I	5155.125	-0.650	-0.642	ab
Fe I	6705.101	-1.496	-1.021	c	Fe I	8699.454	-0.380	-0.329	c	Ni I	5155.762	+0.011	-0.084	abcd
Fe I	6713.745	-1.600	-1.428	b	Fe I	8710.392	-0.646	-0.311	c	Ni I	5435.855	-2.590	-2.495	b
Fe I	6715.383	-1.640	-1.436	ac	Fe I	8838.429	-2.050	-1.938	c	Ni I	5593.733	-0.840	-0.773	b
Fe I	6725.357	-2.300	-2.186	b	Fe II	4416.830	-2.410	-2.524	a	Ni I	5614.768	-0.508	-0.465	a
Fe I	6726.661	-0.829	-0.976	a	Fe II	4491.405	-2.700	-2.504	ab	Ni I	5663.975	-0.430	-0.424	ac
Fe I	6732.065	-2.210	-2.167	b	Fe II	4508.288	-2.250	-2.333	ab	Ni I	5682.198	-0.470	-0.457	b
Fe I	6733.151	-1.580	-1.424	ab	Fe II	4515.339	-2.450	-2.540	ac	Ni I	5694.977	-0.610	-0.626	abc
Fe I	6745.101	-2.160	-2.106	b	Fe II	4520.224	-2.600	-2.475	b	Ni I	5754.655	-2.330	-2.028	ad
Fe I	6750.153	-2.621	-2.629	bc	Fe II	4541.524	-2.790	-3.002	bc	Ni I	5805.213	-0.640	-0.627	abc
Fe I	6752.707	-1.204	-1.199	bc	Fe II	4576.340	-2.920	-2.901	ab	Ni I	5996.727	-1.060	-1.026	b
Fe I	6804.001	-1.496	-1.503	b	Fe II	4620.521	-3.240	-3.199	abc	Ni I	6007.306	-3.330	-3.406	b
Fe I	6806.845	-3.210	-3.124	a	Fe II	4993.358	-3.640	-3.600	ac	Ni I	6053.679	-1.070	-1.019	b
Fe I	6810.263	-0.986	-0.962	ac	Fe II	5132.669	-3.980	-3.917	c	Ni I	6086.276	-0.530	-0.467	ac
Fe I	6820.372	-1.320	-1.125	abc	Fe II	5197.577	-2.100	-2.185	ac	Ni I	6108.107	-2.450	-2.567	ab
Fe I	6828.591	-0.920	-0.821	b	Fe II	5234.625	-2.230	-2.178	ac	Ni I	6111.066	-0.870	-0.845	abc
Fe I	6841.339	-0.750	-0.617	b	Fe II	5256.938	-4.250	-4.055	a	Ni I	6175.360	-0.559	-0.519	bc
Fe I	6843.656	-0.930	-0.821	ab	Fe II	5284.109	-2.990	-2.955	a	Ni I	6176.807	-0.260	-0.265	abcd
Fe I	6999.884	-1.560	-1.386	b	Fe II	5325.553	-3.120	-3.050	bcd	Ni I	6204.600	-1.100	-1.125	abc
Fe I	7038.223	-1.300	-1.164	b	Fe II	5362.869	-2.739	-2.341	a	Ni I	6223.981	-0.910	-0.936	ac
Fe I	7068.410	-1.380	-1.324	bc	Fe II	5414.073	-3.540	-3.447	ac	Ni I	6259.592	-1.400	-1.220	b
Fe I	7086.722	-2.682	-2.497	b	Fe II	5425.257	-3.160	-3.126	abcd	Ni I	6378.247	-0.830	-0.825	ab
Fe I	7090.383	-1.210	-1.079	bc	Fe II	5427.826	-1.664	-1.347	c	Ni I	6482.796	-2.630	-2.825	a
Fe I	7130.922	-0.790	-0.721	c	Fe II	5534.847	-2.730	-2.748	ab	Ni I	6635.118	-0.820	-0.734	ab
Fe I	7132.986	-1.628	-1.607	bc	Fe II	5991.376	-3.540	-3.444	ac	Ni I	6643.629	-2.300	-2.037	abcd
Fe I	7142.503	-0.931	-0.863	bc	Fe II	6084.111	-3.780	-3.724	cd	Ni I	6767.768	-2.170	-2.130	bc
Fe I	7145.316	-1.532	-1.196	c	Fe II	6147.741	-2.721	-2.654	c	Ni I	6772.313	-0.980	-0.991	abc
Fe I	7401.685	-1.599	-1.524	c	Fe II	6149.258	-2.720	-2.633	ac	Ni I	7030.006	-1.860	-1.765	b
Fe I	7411.154	-0.428	-0.214	bc	Fe II	6238.392	-2.630	-2.765	ab	Ni I	7110.892	-2.980	-2.935	b
Fe I	7418.667	-1.376	-1.382	bc	Fe II	6239.366	-4.538	-4.745	a	Ni I	7122.191	+0.040	-0.245	bc
Fe I	7445.746	-0.237	+0.022	b	Fe II	6247.557	-2.310	-2.194	abcd	Ni I	7385.236	-1.970	-1.935	b
Fe I	7453.998	-2.410	-2.294	b	Fe II	6369.462	-4.160	-4.052	ad	Ni I	7393.600	-0.825	-0.126	bc
Fe I	7461.521	-3.580	-3.472	b	Fe II	6432.680	-3.520	-3.485	ab	Ni I	7422.277	-0.140	-0.277	c
Fe I	7481.933	-1.800	-1.689	b	Fe II	6446.410	-1.960	-1.885	b	Ni I	7525.111	-0.546	-0.582	bc
Fe I	7484.297	-1.700	-1.553	b	Fe II	6456.383	-2.100	-1.990	a	Ni I	7555.598	-0.046	+0.061	bc
Fe I	7491.649	-1.014	-0.897	bc	Fe II	7711.723	-2.500	-2.427	b	Ni I	7714.314	-2.200	-1.718	b
Fe I	7568.894	-0.882	-0.774	bc	²⁷ Co I	5352.045	+0.060	-0.029	a	Ni I	7727.613	-0.170	-0.344	bc
Fe I	7583.788	-1.885	-1.925	b	Co I	5647.234	-1.560	-1.670	b	Ni I	7748.891	-0.343	-0.163	b
Fe I	7586.014	-0.871	-0.026	bc	²⁸ Ni I	4331.640	-2.100	-2.076	b	Ni I	7788.936	-2.420	-1.953	bc
Fe I	7710.364	-1.113	-1.071	b	Ni I	4410.512	-1.080	-1.015	b	Ni I	7797.586	-0.262	-0.178	bc
Fe I	7748.269	-1.751	-1.708	b	Ni I	4715.757	-0.320	-0.456	abcd	³⁹ Y II	4883.684	+0.070	+0.163	a
Fe I	7751.137	-0.895	-0.667	b	Ni I	4756.510	-0.270	-0.325	b	Y II	5087.416	-0.170	-0.196	abc
Fe I	7780.552	-2.361	+0.374	b	Ni I	4806.984	-0.640	-0.585	abc	Y II	5200.406	-0.570	-0.792	c